Macromolecules

pubs.acs.org/Macromolecules Article

Enhancement of Mechano-Sensitivity for Spiropyran-Linked Poly(dimethylsiloxane) via Solvent Swelling

Dong Woo Kim, Grigori A. Medvedev, James M. Caruthers, Jun Young Jo, You-Yeon Won,* and Jaewoo Kim*

Cite This: *Macromolecules* 2020, 53, 7954–7961 Read Online

ACCESS | Metrics & More | Article Recommendations | Supporting Information

ABSTRACT: Spiropyran (SP) is a mechanophore that undergoes changes in chemical structure and thus in optical character when subjected to a force. Incorporation of SP into polymer chains enables optical detection of stress/strain and damage in the material under load. However, the mechano-sensitivity of SP-linked polymers is in general insufficient for many applications. Attempts have been made to enhance the mechano-sensitivity of SP-linked polymers via modification of the chemical structure of the SP mechanophore or the mesostructure of the polymer matrix. In the present study, we explore how the mechano-sensitivity of SP incorporated in a poly(dimethylsiloxane) (PDMS) network is influenced by the pre-swelling of PDMS with an organic solvent (xylene). The effect of PDMS swelling on the optical property of the mechanophore was investigated by measuring the fluorescence intensity from the SP-linked PDMS *in situ* during uniaxial deformation using a custom-built opto-mechanical measurement setup. The results suggest that a longer swelling time causes a decrease in the initial fluorescence, a decrease in the activation onset strain, and an increase in the activation slope, resulting in enhanced apparent mechano-sensitivity. For instance, the 15 min pre-swollen SP-linked PDMS showed an 8.3-fold increase in mechano-sensitivity relative to the unswollen reference. Such effect is not limited to uniaxial extension but also observed in other modes of deformation, such as compression and bending. When corrected against the variation in sample thickness during uniaxial extension, and pre-strain and initial fluorescence intensity due to solvent swelling, the SP fluorescence intensity vs true strain (or chain entropy) curves obtained at various degrees of initial swelling collapse into a single curve, which suggests that the swelling-enhanced mechano-sensitivity is due to the pre-strain of the network and a decrease in initial fluorescence intensity caused by the pre-swelling.

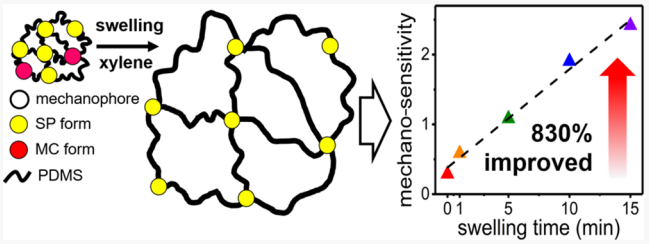

Downloaded via PURDUE UNIV on November 29, 2020 at 03:48:50 (UTC).
See https://pubs.acs.org/sharingguidelines for options on how to legitimately share published articles.

INTRODUCTION

Mechano-chromic polymers exhibit changes in optical properties, such as light emission intensity and/or wavelength under mechanical deformation and have potential for applications in such areas such as stress/strain mapping, damage detection, and anti-counterfeiting.[1−7] One typical method for preparing mechano-chromic polymers is to incorporate force-responsive moieties, called mechanophores, into polymer chains. Spiropyran (SP) is currently one of the most popular mechanophores. When an external force is applied, SP undergoes a reversible chemical transformation into merocyanine (MC) via a ring-opening cleavage of a C−O bond (see Figure 1), resulting in changes in absorbance and fluorescence characteristics;[8] SP is originally colorless (or pale yellow) and non-fluorescent, whereas MC is dark purple (or blue) and highly fluorescent, producing emission at wavelengths between 550 and 700 nm.[9] These changes are typically detectable even with the naked eye. As shown in Figure 1, the SP to MC transformation is reversible, where MC returns to SP upon illumination by visible light.

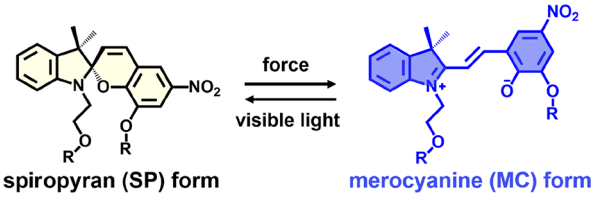

Figure 1. Chemical structure of the spiropyran (SP) mechanophore and its transformation into the merocyanine (MC) form.

Since the mechano-chromic property of SP-linked poly(methyl acrylate) was first demonstrated in 2007,[16] the SP mechanophore has been applied to a wide variety of polymers, including poly(carbonate),[11] poly(caprolactone),[12,13] poly-

Received: May 4, 2020
Revised: August 28, 2020
Published: September 10, 2020

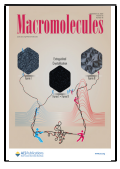

ACS Publications © 2020 American Chemical Society

https://dx.doi.org/10.1021/acs.macromol.0c00985
Macromolecules 2020, 53, 7954–7961

(methyl methacrylate),[10,14,15] poly(urethane) (PU),[17−19] and poly(dimethylsiloxane) (PDMS).[20−22] SP-linked ductile/stretchable polymers are potentially useful for wearable sensors, e-skins, flexible electronics, and bio-mimics.[23−25] However, relatively low mechano-sensitivities, i.e., low sensitivities to mechanical stimuli (stress/strain) of SP-linked polymers have been recognized as a limiting factor for their use in these applications. In rubbery polymer networks, SP is converted into MC only at high strains (e.g., >50% in SP-linked PDMS and >500% in SP-linked PU);[26,27] in ductile/rubbery polymers, which are easily deformed under small loads, only a small fraction of the applied force is transmitted to the SP links, resulting in a poor sensitivity to deformation.[28] Therefore, the development of SP-linked polymers with improved mechano-sensitivities is highly desirable for many applications.

Several attempts to improve the mechano-sensitivity of SP-linked polymers have been reported. One approach is to modify the chemical structure of the SP mechanophore. Gossweiler and co-workers synthesized two different variants of SP with an identical functional group attached at two different sites, and their single molecule force spectroscopy measurements demonstrated that different amounts of force are required to induce the SP to MC transition between the two SP derivatives.[29] Barbee and co-workers investigated the effect of the substituent on the mechanochemical reactivity of SP.[30] They found that with more electron withdrawing substituent, a smaller force is required to induce the SP-MC transition. Another avenue explored is the modification of the polymer matrix so that an external force is more effectively transmitted to the SP linkages. Chen and co-workers incorporated ureidopyrimidinone (UP) into SP-linked PU so that the resulting supramolecular interaction enables more efficient force transfer and thus improves the mechano-sensitivity.[27] Park and co-workers created a hierarchical nanoparticle-in-micropore structure in SP-linked PDMS, in which the mechano-sensitivity is enhanced due to the structure-induced stress concentration.[23] Beiermann and co-workers achieved a mechano-activation of a glassy polymer (PMMA) at room temperature using methanol as a plasticizer.[32] Raisch and co-workers, using electrospinning, fabricated highly oriented poly(SP-alt-C_{10}) nanofibers, which exhibited an enhanced mechano-sensitivity in the direction of the nanofiber orientation.[31] In addition, Qiao and co-workers incorporated SP into a polyacrylate multi-network structure and showed that its mechanochromic sensitivity can be regulated by the variation of a network composition.[34]

In the present study, we explore solvent pre-swelling as means to enhance the mechano-sensitivity of a SP-linked polymer network. Divinyl functionalized SP was covalently incorporated into a PDMS network.[20] The PDMS swelling degree was controlled by varying the time of swelling in a solvent, xylene. The mechano-response of SP-linked PDMS was characterized *in situ* by the measurement of the fluorescence intensity during a uniaxial tensile test using a custom-built opto-mechanical measurement setup. The results suggest that the mechano-sensitivity of SP-linked PDMS increases linearly with swelling time. This swelling-induced mechano-sensitivity enhancement was not limited to extension but also observed in compression and bending. We found that the fluorescence intensity vs true strain (or chain entropy) curves obtained at various degrees of pre-swelling collapse onto a single curve when the fluorescence intensity is corrected for the decrease in thickness of the specimen during stretching and the pre-strain and initial fluorescence intensity caused by swelling.

EXPERIMENTAL SECTION

All chemical reagents used in this study were purchased from Sigma-Aldrich. Organic solvents were purified by distillation on CaH_2 before use. First, dihydroxyl SP (1′-(2-hydroxyethyl)-3′,3′-dimethyl-6-nitrospiro[chromene-2,2′-indolin]-8-ol) was synthesized using a published procedure.[10,21] The hydroxyl groups of the SP were then converted into vinyl groups using the procedure of Gossweiler and co-workers[20] (with minor modifications). Briefly, 1.48 g of dihydroxyl SP and 0.88 g of 4-dimethylamino pyridine were dissolved in 50 mL of anhydrous THF, and then 1.90 g of 4-pentenoic anhydride was added. After stirring at room temperature in a nitrogen atmosphere for 24 h, the solution mixture was purified by flowing through a basic alumina column using ethyl acetate and n-hexane (1:3 v/v) as the eluent, dried in vacuum, and recrystallized from hot hexane. The resulting yellow crystals were separated with filter paper, washed with cold hexane, and then dried overnight in a vacuum oven at 60 °C. The final divinyl functionalized SP mechanophore exhibited green color. The detailed synthesis scheme and NMR spectra of divinyl SP are presented in Scheme S1 and Figure S1 in the Supporting Information, respectively.

SP was chemically incorporated into PDMS via hydrosilylation. Divinyl functionalized SP (0.12 g) was completely dissolved in 1.6 mL of xylene in a 70 mL glass vial, and then 16.0 g of Sylgard 184 base (Dow Corning, USA) was added. The solution was vigorously mixed for 5 min using a vortex mixer (Vortex Genie 2, Scientific Industries Inc., USA) until the color of the solution changed from blue to pale red. Next, 1.6 g of the Sylgard 184 curing agent was added, and the solution was agitated with a vortex mixer until the color turned to pale yellow in approximately 5 min. After sonication for 3 min to remove bubbles, the polymerization reaction was carried out between a pair of Pyrex glass plates fixed with clamps using a Teflon-encapsulated Viton O-ring as a spacer. Curing conditions were 70 °C for 4 h followed by 25 °C for 12 h. The resulting SP-linked PDMS sheet was removed from the glass plates and cut into a dog-bone shape using a laser cutting system (ILS 12.150D, Universal Laser Systems, USA). Specimens were stored in a desiccator under dark conditions for 24 h before performing the swelling and opto-mechanical experimentation. The specific dimensions of the dog-bone specimen are summarized in Figure S2 in the Supporting Information. SP-linked PDMS samples with different degrees of swelling were produced by immersing the dog-bone specimens in xylene for different amounts of time, i.e., 0, 1, 5, 10, and 15 min. Following swelling over a specified time, the specimen was taken out of xylene and immediately subjected to mechanical testing. Since the specimen underwent an isotropic expansion during solvent swelling, its volume expansion ratio was calculated as the cube of the extension ratio.

The mechano-response of SP-linked PDMS was measured using a custom-built opto-mechanical setup, in which the full-field fluorescence intensity of a dog-bone specimen was measured *in situ* under deformation, as schematically shown in Figure 2. Uniaxial extension

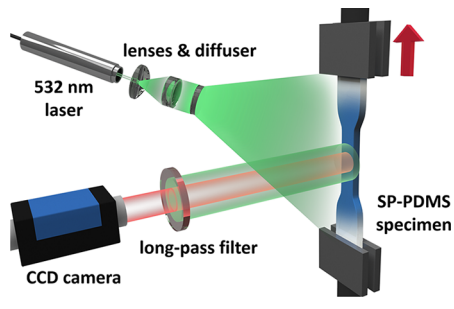

Figure 2. Schematic of the custom-built opto-mechanical measurement set-up used in this study.

https://dx.doi.org/10.1021/acs.macromol.0c00985
Macromolecules 2020, 53, 7954−7961

experiments were performed at a constant strain rate of 0.007 s^{-1} at 25 °C using an Instron 5567A universal testing machine equipped with a 100 N capacity load cell. Pneumatic grips were employed to avoid slippage during extension. The force and crosshead displacement were converted to the true stress and true strain (Henky strain), respectively, based on the instantaneous cross-sectional area and length of the specimen. As shown in Figure 2, light from a 532 nm laser (CPS532, Thorlabs Inc., USA, 5 mW) passed through optical components consisting of a concave lens (LC2679-A, Thorlabs Inc., USA), a convex lens (LA1433-A, Thorlabs Inc., USA), and an engineering diffuser (ED1-S20-MD, Thorlabs Inc., USA) and subsequently illuminated a dog-bone specimen with a beam width greater than the width of the specimen and a uniform intensity distribution. The intensity of the fluorescence emitted from the illuminated SP-linked PDMS specimen was measured using a CCD detector (Prosilica GT2750, Allied Vision Technologies GmbH, Germany) after passing through a 575 nm long-pass filter (OD4-575 nm 50 mm, Edmund Optics, USA) to eliminate scattering and reflection. Fluorescence images of the specimen were recorded every 2.5 s with an exposure time of 0.6 s during extension. ImageJ software was used to quantify the average fluorescence intensity from the region of interest (ROI), which covered approximately 50% of the gauge area of the specimen. All experiments were performed inside a rubber-coated black-out fabric (BK5, Thorlabs Inc., USA) to block external light.

RESULTS AND DISCUSSION

Swelling Behavior of SP-Linked PDMS. Figure 3a displays photos of SP-linked PDMS dog-bone specimens pre-

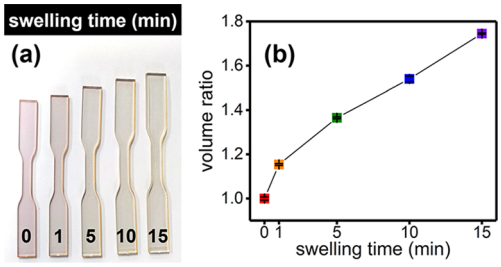

Figure 3. (a) Photographic images and (b) volume expansion ratio vs swelling time relationships for SP-linked PDMS specimens prepared at different swelling times.

swollen in xylene for different time periods. As the swelling time was increased from 0 to 1, 5, 10, and 15 min,, an increasing amount of xylene was absorbed by the specimen, resulting in an increase in its dimensions (length, width, and thickness). At the same time, the color of the SP-linked PDMS changed from red to pale yellow (or colorless) with increase in swelling time. This result is different from that reported by Lee and co-workers.[33] This is because the SP mechanophore preferentially exists in the yellow SP form rather than in the red MC form in a nonpolar solvent such as xylene. The solvatochromic characteristics of divinyl SP in several different solvents (i.e., xylene, toluene, chloroform, acetone, and methanol in the order of an increasing polarity) are demonstrated in Figure S4 in the Supporting Information. As shown in the figure, the color of the SP changed from colorless to deep red (or purple) as the polarity of the solvent was increased, i.e., as the solvent was switched from xylene to toluene, to chloroform, to acetone, and to methanol. Figure 3b shows the volume change of the specimen as a function of the swelling time. Following the rapid initial expansion, a nearly constant rate of volume increase was observed up to 15 min; at 15 min, the specimen volume increased by a factor of 1.75 relative to the unswollen volume. When SP-linked PDMS was pre-swollen longer than 15 min, the samples could not be used for mechanical testing because they crumbled too easily.

Dependence of Mechanical and Mechano-Chemical Response of SP-Linked PDMS on Swelling Time. The effects of pre-swelling on the mechanical and mechano-chemical properties of SP-linked PDMS were investigated using a custom-built opto-mechanical setup, in which the fluorescence intensity from the SP-linked PDMS specimen was recorded *in situ* during uniaxial extension. Figure 4a displays

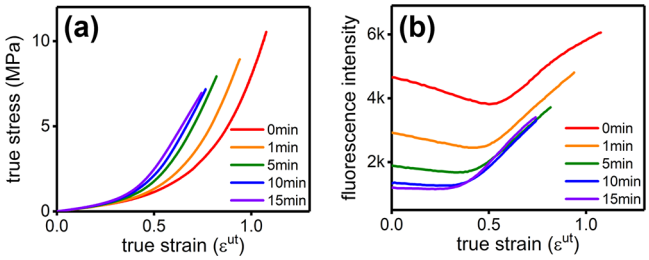

Figure 4. (a) Stress vs strain dependence and (b) fluorescence intensity vs strain dependence for various pre-swollen SP-linked PDMS specimens. ε^{ut} denotes the true strain in uniaxial extension.

the constant strain rate stress vs strain curves for pre-swollen SP-linked PDMS samples prepared at different swelling times. All samples exhibited a typical mechanical response for rubbery polymers, that is, the linear increase in stress at small strains followed by the nonlinear strain hardening at large strains. The increased pre-swelling caused the strain-hardening behavior to begin at a lower strain, resulting in generally higher stresses in the high strain regime. For instance, the 0, 1, 5, 10, and 15 min pre-swollen samples exhibited true stresses of 2.5, 3.4, 5.0, 5.7, and 6.1 MPa, respectively, at a true strain of 0.7. Also, a longer pre-swelling time decreased the fracture strain (Figure 4a).

Figure 4b displays the fluorescence intensities of the pre-swollen SP-linked PDMS samples measured *in situ* during uniaxial extension as functions of strain. A similar shape of the fluorescence intensity vs strain curve was observed for all pre-swelling times; specifically, the fluorescence signal initially declined at low strains but subsequently rose at strains higher than a critical value. The initial decrease in fluorescence intensity is attributed to the decrease in thickness of the SP-linked PDMS specimen caused by the Poisson's effect. Only when a sufficient amount of deformation is applied, the SP mechanophores start experiencing sufficient stretching forces and undergo transformation into the MC isomers, resulting in an increase in fluorescence. As shown in Figure 4b, smaller pre-swelling resulted in an increasingly more V-shaped fluorescence curve. As the amount of pre-swelling increased, the initial fluorescence intensity was reduced, and at the same time the critical strain marking the onset of fluorescence activation also decreased. SP-linked PDMS samples with longer pre-swelling times exhibited steeper slopes for the fluorescence intensity vs strain curves at high strains.

Mechano-Sensitivities of Pre-Swollen SP-Linked PDMS Samples. The data shown in Figure 4b were further analyzed to produce plots of the initial (pre-extension) fluorescence intensity, the strain at the onset of fluorescence activation, and the post-activation slope of the fluorescence intensity vs strain curve as functions of the pre-swelling time (presented in Figure 5a–c, respectively). The decrease in the initial fluorescence intensity with increasing swelling time

https://dx.doi.org/10.1021/acs.macromol.0c00985
Macromolecules 2020, 53, 7954–7961

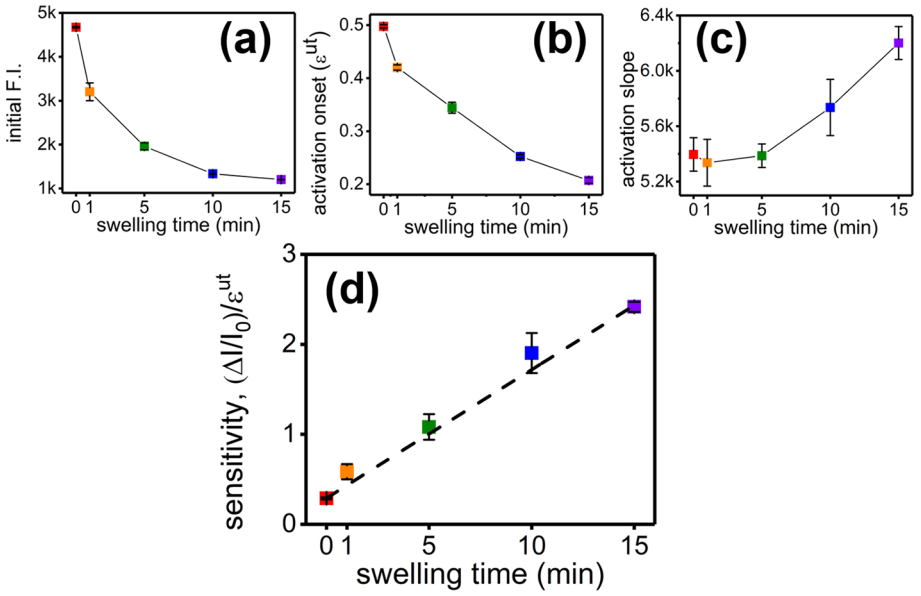

Figure 5. (a) Initial fluorescence intensities, (b) activation onset strains, (c) post-activation fluorescence slopes, and (d) strain sensitivity factors of solvent-swollen SP-linked PDMS specimens prepared at different pre-swelling times.

(Figure 5a) is due to a shift in equilibrium between SP (colorless/yellow) and MC (blue/purple) toward SP in nonpolar xylene. The activation onset strain is defined as the critical strain at which the fluorescence intensity begins to rise during extension and was determined as the point at which the derivative of the fluorescence intensity with respect to the strain becomes equal to zero. As the pre-swelling time was increased, the activation onset strain was found to decrease (Figure 5b); for instance, when the SP-linked PDMS sample was pre-swollen for 15 min, the activation onset strain was reduced to 0.21 (from 0.50 for the unswollen sample). The activation slope was determined from the linear region of the fluorescence intensity vs strain plot, post the activation onset point. As shown in Figure 5c, the activation slope was constant for samples with small degrees of pre-swelling (at swelling times up to 5 min) but increased with swelling time in highly pre-swollen samples. The decrease in the initial fluorescence intensity and the activation onset strain and the increase in the activation slope with increased pre-swelling all positively contribute to an enhancement of the mechano-sensitivity of SP-linked PDMS (Figure 5d). First, the decrease in the initial fluorescence intensity indicates an increase in the SP to MC ratio, which means that an increased amount of active mechanophores (SP) becomes available for mechano-sensing. Second, the decrease in the activation onset strain enables detection of smaller deformations. Finally, a higher activation slope leads to a higher intensity of fluorescence signal for a given mechanical load.

For the SP-linked PDMS samples prepared at different pre-swelling times, the strain sensitivity factors were calculated using the following equation[23]

$$\text{strain sensitivity factor} = \frac{(\Delta I/I_0)}{\varepsilon^{ut}} \quad (1)$$

where I_0 denotes the initial fluorescence intensity, and ΔI denotes the change in the fluorescence intensity relative to I_0 at the point of sample failure. The estimated values of the sensitivity factors were 0.3, 0.5, 1.2, 2.1, and 2.5, for the 0, 1, 5, 10, and 15 min pre-swollen samples (Figure 5d), respectively, suggesting a linear relationship between the sensitivity factor and the pre-swelling time. Particularly, the 15 min pre-swollen SP-linked PDMS sample exhibited an 8.3-fold enhancement of the mechano-sensitivity relative to the non-swollen reference. The mechano-sensitivity enhancement observed after the pre-swelling treatment can thus be understood as being caused by the combined effects of decreased initial fluorescence intensity, decreased activation onset strain, and increased activation slope.

The mechano-sensitivity enhancement observed in the 15 min pre-swollen SP-linked PDMS sample was further validated with other types of mechanical deformation. As shown in Figure 6a, the pale red color of the unswollen specimen

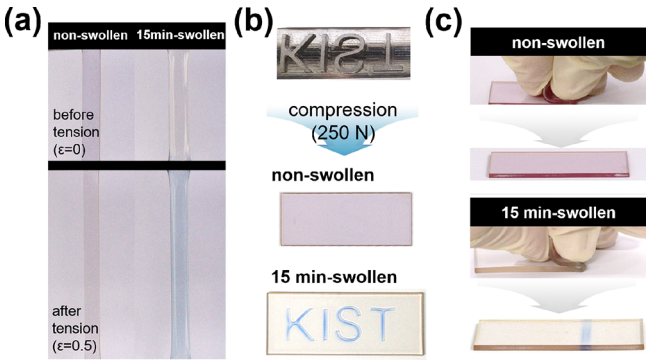

Figure 6. Comparison of the mechano-sensitivities of the non-swollen and 15 min pre-swollen SP-linked PDMS specimens under different types of deformation modes: (a) uniaxial extension, (b) compression, and (c) bending.

remained unchanged even after uniaxial stretching, indicating a poor mechano-sensitivity of the unswollen material. In contrast, the 15 min pre-swollen specimen exhibited a significant change from colorless to blue when the same amount of tensile strain was applied, indicating a significant enhancement of the mechano-sensitivity upon pre-swelling. Figure 6b,c demonstrates similar results for the 15 min pre-

https://dx.doi.org/10.1021/acs.macromol.0c00985
Macromolecules 2020, 53, 7954−7961

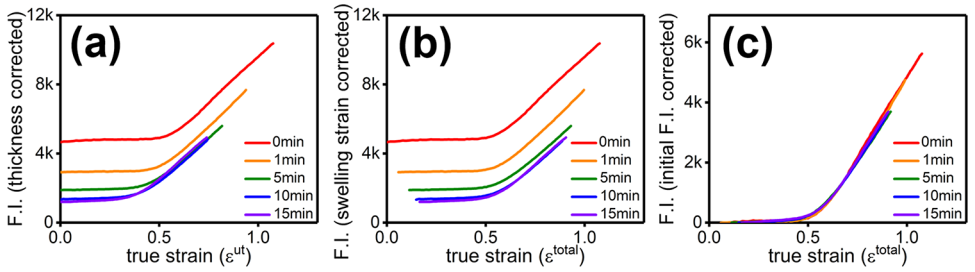

Figure 7. Original fluorescence intensity vs true strain curves shown in Figure 4b have been rescaled to take into account the (a) variation of the thickness of the specimen during the uniaxial deformation, (b) additional strain caused by the solvent pre-swelling, and (c) difference in the initial fluorescence intensity among specimens prepared at different pre-swelling times. ε^{ut} denotes the true strain caused by uniaxial extension. ε^{total} denotes the total strain, which is the sum of the uniaxial strain and the pre-strain caused by the solvent swelling.

swollen sample under compressive and bending loads, respectively.

Origin of Swelling-Induced Mechano-Sensitivity Enhancement. To better understand the exact origin of the pre-swelling-induced mechano-sensitivity enhancement, the original fluorescence intensity vs true strain data (Figure 4b) were corrected for the variation of the sample thickness during the uniaxial extension, the pre-strain caused by the solvent swelling, and the initial level of fluorescence prior to uniaxial deformation. The resulting corrected fluorescence intensity vs strain curves are presented in Figure 7a–c.

Since the area of the specimen from which the fluorescence intensity was measured was always constant, the total number of the SP or MC moieties probed within the illumination volume changed in proportion to the change in the thickness of the specimen during the uniaxial deformation. Therefore, the thickness change has to be accounted for to keep the number of SP moieties the same during deformation. The change in thickness of the specimen during the uniaxial extension can be estimated using the equation

$$\Delta d = -d_0\left(1 - \left(1 + \frac{\Delta L}{L_0}\right)^{-\nu}\right) \tag{2}$$

where d_0 and L_0 denote the initial thickness and length of the specimen, respectively, and Δd and ΔL denote the changes in thickness and length of the specimen, respectively, that occur during the uniaxial deformation; ν denotes the Poisson's ratio of SP-linked PMDS. A value of $\nu = 0.5$ was used assuming that xylene-swollen SP-linked PDMS behaves like an ideal rubber. Thus, the thickness-corrected fluorescence intensity was calculated as

$$\begin{aligned}&\text{thickness corrected fluorescence intensity}\\ &= \frac{\text{F. intensity}}{\left(\frac{\Delta d + d_0}{d_0}\right)}\\ &= \frac{\text{F. intensity}}{\left(1 + \frac{\Delta L}{L_0}\right)^{-\nu}}\end{aligned} \tag{3}$$

The thickness-corrected fluorescence intensity vs true strain curves are shown in Figure 7a. As seen in the figure, the thickness-corrected fluorescence intensity is constant at small strains, i.e., at strains lower than the onset of fluorescence activation and only begins to increase with deformation at large strains. The slopes of the high-strain portions of the intensity vs strain curves generally became steeper after the thickness corrections. However, the slope increase due to the thickness correction was greater for shorter pre-swelling times so that all fluorescence intensity vs strain curves exhibited comparable post-activation slopes after correction for the variation in thickness of the specimen (Figure 7a). Details of the calculation of the activation slopes are presented in Section 6 of the Supporting Information. Further, the total strain experienced by the specimen ε^{total} was estimated by adding the isotropic pre-strain caused by swelling ε^{sw} to the uniaxial tensile strain ε^{ut}, and the fluorescence intensity data were replotted in terms of ε^{total} in Figure 7b. As shown in the figure, the longer the pre-swelling time, the greater the pre-strain became due to the expansion of the specimen. Thus, when corrected against swelling strain, the fluorescence intensity vs true strain curve was shifted more to the right. After this correction, we found that the values of the fluorescence onset ("activation") strains coincide for all pre-swelling times (Figure 7b). Details of the calculation of the onset strains are described in Section 6 of the Supporting Information. Lastly, to take into account the amount of the MC moieties that existed in the specimen prior to the uniaxial deformation, that is, to measure only the amount of MC produced from SP during the uniaxial tensile test, we further subtracted the initial fluorescence intensity from the overall fluorescence intensity (that is, the fluorescence intensity curves were vertically shifted downward so that y-intercepts are set to zero for all curves). This procedure assumes that the initial SP/MC ratio does not affect the SP-MC conversion process. The final shifted fluorescence intensity curves are presented in Figure 7c. As shown in the figure, all curves superimpose onto a single curve within a relative standard deviation (for the area under the curve) of about 2.1%, which strongly supports the analysis described in this paragraph.

We would like to point out that the true strain used above only considers the deformation of the specimen along the direction of uniaxial extension. However, solvent swelling typically produces an isotropic expansion of the specimen; uniaxial extension causes an extension of the material along the longitudinal (tensile) axis, whereas it causes a contraction of the sample along the transverse axes. Therefore, the uniaxial strain quantity might not precisely capture the full effect of deformation experienced by the mechanophores. For this reason, we evaluated the respective entropy changes associated with the solvent pre-swelling and uniaxial extension processes using the following equations, respectively,

$$\Delta S^{sw} = -\frac{N_t k}{2}(3\lambda_{sw}^2 - 3 - \ln \lambda_{sw}^3) \tag{4}$$

https://dx.doi.org/10.1021/acs.macromol.0c00985
Macromolecules 2020, 53, 7954–7961

$$\Delta S^{ut} = -\frac{N_t k}{2}\lambda_{sw}^2\left(\lambda_{ut}^2 - 3 + \frac{2}{\lambda_{ut}}\right) \quad (5)$$

$$\Delta S^{total} = \Delta S^{sw} + \Delta S^{ut} \quad (6)$$

where λ_{sw} and λ_{ut} denote the extension ratios for the solvent pre-swelling and uniaxial tension, respectively, and N_t denotes the total number of elastic strands, and k is the Boltzmann constant. The above equations assume that the network is composed of Gaussian strands; see Section 5 in the Supporting Information for derivations. Figure 8 displays plots of the corrected fluorescence intensity vs total entropy change for the system. As shown in the figure, all curves overlap with a relative standard deviation for the curve area of about 5.6%. This result suggests that the net overall deformations of the mechanophores in the transverse directions are negligible, because of the near cancellation of the effects of the initial volume expansion during pre-swelling and the contraction in the transverse directions caused by the uniaxial elongation.

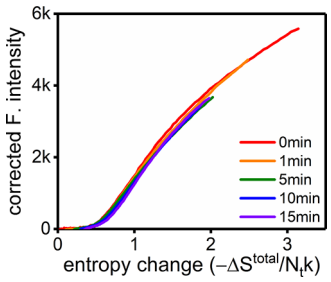

Figure 8. Corrected fluorescence intensity vs total entropy change for the system curves for pre-swollen SP-linked PDMS specimens prepared at different swelling times.

The results of the above analyses (Figures 7 and 8) suggest that the pre-swelling-induced mechano-sensitivity enhancement of SP-linked PDMS is due to the combined effects of thickness reduction, pre-swelling deformation, and decreased initial fluorescence intensity. The unswollen specimen showed the highest initial fluorescence intensity, and the greatest decrease in fluorescence intensity due to reduced thickness under uniaxial extension (Figure 4b). The intensity decrease due to the thickness decrease was the smallest for the 15 min pre-swollen specimen (Figure 4b). The greater the pre-swelling, the steeper the slope of the fluorescence intensity vs tensile strain curve became (i.e., the greater the mechano-sensitivity became) (Figure 4b), because a smaller initial fluorescence intensity causes a reduced decrease in fluorescence due to a further decrease in thickness. The solvent absorption created a pre-strain in the SP-linked PDMS network. As a result, a smaller amount of additional strain was necessary to induce the mechano-chemical activation of the SP mechanophores (Figure 7b). The solvent-induced mechano-sensitivity enhancement is attributed to the decreased initial fluorescence intensity (the shift of the SP-MC equilibrium toward the SP state), the decreased sensitivity of the fluorescence intensity to the thickness of the specimen, and the pre-strain created due to the solvent swelling.

CONCLUSIONS

In the present study, we explored whether solvent pre-swelling can be used as means to enhance the mechano-sensitivity of SP-linked PDMS. SP-linked PDMS was synthesized by covalently incorporating divinyl functionalized SP linkages into a cross-linked PDMS network. Pre-swollen SP-linked PDMS samples with different degrees of swelling were produced by exposing SP-linked PDMS to a nonpolar solvent (xylene) for different periods of time (0, 1, 5, 10, and 15 min). The mechano-responses of these samples were investigated using an inhouse-developed opto-mechanical measurement setup that enabled *in situ* measurement of the fluorescence intensity from a SP-linked PDMS specimen during uniaxial extension. We found that the mechano-sensitivity of solvent-swollen SP-linked PDMS increased in proportion to the pre-swelling time. The swelling-induced mechano-sensitivity enhancement was due to the combined effects of decreased initial fluorescence intensity, decreased fluorescence onset strain, and increased post-activation florescence intensity slope. The 15 min pre-swollen SP-linked PDMS specimen, for instance, exhibited an 8.3-fold increase in mechano-sensitivity relative to the unswollen state. A similar, swelling-induced enhancement of the mechano-sensitivity of SP-linked PDMS networks was also observed with other types of deformation such as compression and bending. When rescaled to take into account the variation of the specimen thickness during uniaxial extension and the differences in the magnitude of the pre-strain caused by the solvent swelling and in the initial fluorescence intensity, the fluorescence intensity vs strain curves collapsed onto a single curve for all values of pre-swelling time. This result suggests that the swelling-induced mechano-sensitivity enhancement is due to the combined effects of the decreased initial fluorescence intensity, the decreased sensitivity of the fluorescence intensity to the thickness of the specimen ,and the additional strain caused by the solvent pre-swelling. The results of this study provide insights on how solvent pre-swelling could be used as means to enhance the mechano-sensitivity of SP-linked polymer networks.

ASSOCIATED CONTENT

Supporting Information

The Supporting Information is available free of charge at https://pubs.acs.org/doi/10.1021/acs.macromol.0c00985.

Synthesis scheme and 1H NMR spectra for divinyl functionalized SP, dimensions of dog-bone shaped SP-linked PDMS specimens, solvatochromism of divinyl functionalized SP, calculation of the entropy changes per elastic strand associated with solvent swelling and uniaxial extension of an ideal network, evolution of fluorescence intensity with time with no external force at five different pre-swelling times, UV−vis absorption spectra of SP-linked PDMS in the presence and absence of xylene (PDF)

AUTHOR INFORMATION

Corresponding Authors

You-Yeon Won − *Davidson School of Chemical Engineering, Purdue University, West Lafayette, Indiana 47907, United States*; Email: yywon@purdue.edu.

Jaewoo Kim − *Structural Composite Research Center, Institute of Advanced Composite Materials, Korea Institute of Science and Technology (KIST), Wanju-gun, Jeonbuk 55324, Republic of Korea*; orcid.org/0000-0002-0967-0882; Email: jaewoo96@kist.re.kr.

https://dx.doi.org/10.1021/acs.macromol.0c00985
Macromolecules 2020, 53, 7954−7961

Authors

Dong Woo Kim − *Structural Composite Research Center, Institute of Advanced Composite Materials, Korea Institute of Science and Technology (KIST), Wanju-gun, Jeonbuk 55324, Republic of Korea*

Grigori A. Medvedev − *Davidson School of Chemical Engineering, Purdue University, West Lafayette, Indiana 47907, United States*

James M. Caruthers − *Davidson School of Chemical Engineering, Purdue University, West Lafayette, Indiana 47907, United States*

Jun Young Jo − *Structural Composite Research Center, Institute of Advanced Composite Materials, Korea Institute of Science and Technology (KIST), Wanju-gun, Jeonbuk 55324, Republic of Korea;* orcid.org/0000-0001-6117-6104

Complete contact information is available at: https://pubs.acs.org/10.1021/acs.macromol.0c00985

Author Contributions

The manuscript was written through collaboration among all authors. All authors approved the final version of the manuscript.

Notes

The authors declare no competing financial interest.

■ ACKNOWLEDGMENTS

This study was supported by the Korea Institute of Science and Technology (KIST) Institutional Program (2Z06050). In addition, this material is based upon work supported by the Ministry of Trade, Industry & Energy of Korea under Industrial Technology Innovation Program (10082586). Y.Y.W. is grateful for funding from US NSF (CBET-1803968) and from ACS PRF (602033-ND7).

■ REFERENCES

(1) Roberts, D. R.; Holder, S. J. Mechanochromic systems for the detection of stress, strain and deformation in polymeric materials. *J. Mater. Chem.* **2011**, *21*, 8256−8268.

(2) Li, M.; Zhang, Q.; Zhou, Y.-N.; Zhu, S. Let spiropyran help polymers feel force! *Prog. Polym. Sci.* **2018**, *79*, 26−39.

(3) Zhang, R.; Wang, Q.; Zheng, X. Flexible mechanochromic photonic crystals: routes to visual sensors and their mechanical properties. *J. Mater. Chem. C* **2018**, *6*, 3182−3199.

(4) Hu, J.; Liu, S. Responsive polymers for detection and sensing applications: current status and future developments. *Macromolecules* **2010**, *43*, 8315−8330.

(5) Celestine, A. D. N.; Sottos, N. R.; White, S. R. Strain and stress mapping by mechanochemical activation of spiropyran in poly (methyl methacrylate). *Strain* **2019**, *55*, No. e12310.

(6) Kim, J. W.; Jung, Y.; Coates, G. W.; Silberstein, M. N. Mechanoactivation of spiropyran covalently linked PMMA: effect of temperature, strain rate, and deformation mode. *Macromolecules* **2015**, *48*, 1335−1342.

(7) Jo, J. Y.; Jang, H. G.; Jung, Y. C.; Lee, D. C.; Kim, J. Revealing the Dependence of Molecular-Level Force Transfer and Distribution on Polymer Cross-Link Density via Mechanophores. *ACS Macro Lett.* **2019**, *8*, 882−887.

(8) Klajn, R. Spiropyran-based dynamic materials. *Chem. Soc. Rev.* **2014**, *43*, 148−184.

(9) Chen, J.; Zeng, F.; Wu, S. Construction of energy transfer systems within nanosized polymer micelles and their fluorescence modulation properties. *ChemPhysChem* **2010**, *11*, 1036−1043.

(10) Davis, D. A.; Hamilton, A.; Yang, J.; Cremar, L. D.; Van Gough, D.; Potisek, S. L.; Ong, M. T.; Braun, P. V.; Martínez, T. J.; White, S. R.; Moore, J. S.; Sottos, N. R. Force-induced activation of covalent bonds in mechanoresponsive polymeric materials. *Nature* **2009**, *459*, 68.

(11) Vidavsky, Y.; Yang, S. J.; Abel, B. A.; Agami, I.; Diesendruck, C. E.; Coates, G. W.; Silberstein, M. N. Enabling Room-Temperature Mechanochromic Activation in a Glassy Polymer: Synthesis and Characterization of Spiropyran Polycarbonate. *J. Am. Chem. Soc.* **2019**, *141*, 10060−10067.

(12) Peterson, G. I.; Larsen, M. B.; Ganter, M. A.; Storti, D. W.; Boydston, A. J. 3D-printed mechanochromic materials. *ACS Appl. Mater. Interfaces* **2014**, *7*, 577−583.

(13) O'Bryan, G.; Wong, B. M.; McElhanon, J. R. Stress sensing in polycaprolactone films via an embedded photochromic compound. *ACS Appl. Mater. Interfaces* **2010**, *2*, 1594−1600.

(14) Beiermann, B. A.; Kramer, S. L. B.; May, P. A.; Moore, J. S.; White, S. R.; Sottos, N. R. The Effect of Polymer Chain Alignment and Relaxation on Force-Induced Chemical Reactions in an Elastomer. *Adv. Funct. Mater.* **2014**, *24*, 1529−1537.

(15) Kingsbury, C. M.; May, P. A.; Davis, D. A.; White, S. R.; Moore, J. S.; Sottos, N. R. Shear activation of mechanophore-crosslinked polymers. *J. Mater. Chem.* **2011**, *21*, 8381−8388.

(16) Potisek, S. L.; Davis, D. A.; Sottos, N. R.; White, S. R.; Moore, J. S. Mechanophore-linked addition polymers. *J. Am. Chem. Soc.* **2007**, *129*, 13808.

(17) Zhang, H.; Chen, Y.; Lin, Y.; Fang, X.; Xu, Y.; Ruan, Y.; Weng, W. Spiropyran as a mechanochromic probe in dual cross-linked elastomers. *Macromolecules* **2014**, *47*, 6783−6790.

(18) Hong, G.; Zhang, H.; Lin, Y.; Chen, Y.; Xu, Y.; Weng, W.; Xia, H. Mechanoresponsive healable metallosupramolecular polymers. *Macromolecules* **2013**, *46*, 8649−8656.

(19) Lee, C. K.; Davis, D. A.; White, S. R.; Moore, J. S.; Sottos, N. R.; Braun, P. V. Force-induced redistribution of a chemical equilibrium. *J. Am. Chem. Soc.* **2010**, *132*, 16107−16111.

(20) Gossweiler, G. R.; Hewage, G. B.; Soriano, G.; Wang, Q.; Welshofer, G. W.; Zhao, X.; Craig, S. L. Mechanochemical activation of covalent bonds in polymers with full and repeatable macroscopic shape recovery. *ACS Macro Lett.* **2014**, *3*, 216−219.

(21) Kim, T. A.; Robb, M. J.; Moore, J. S.; White, S. R.; Sottos, N. R. Mechanical Reactivity of Two Different Spiropyran Mechanophores in Polydimethylsiloxane. *Macromolecules* **2018**, *51*, 9177−9183.

(22) Rohde, R. C.; Basu, A.; Okello, L. B.; Barbee, M. H.; Zhang, Y.; Velev, O. D.; Nelson, A.; Craig, S. L. Mechanochromic composite elastomers for additive manufacturing and low strain mechanophore activation. *Polym. Chem.* **2019**, *10*, 5985−5991.

(23) Park, J.; Lee, Y.; Barbee, M. H.; Cho, S.; Cho, S.; Shanker, R.; Kim, J.; Myoung, J.; Kim, M. P.; Baig, C.; Craig, S. L.; Ko, H. Hierarchical Nanoparticle-in-Micropore Architecture for Enhanced Mechanosensitivity and Stretchability in Mechanochromic Electronic Skins. *Adv. Mater.* **2019**, *31*, 1808148.

(24) Barbee, M. H.; Mondal, K.; Deng, J. Z.; Bharambe, V.; Neumann, T. V.; Adams, J. J.; Boechler, N.; Dickey, M. D.; Craig, S. L. Mechanochromic Stretchable Electronics. *ACS Appl. Mater. Interfaces* **2018**, *10*, 29918−29924.

(25) Wang, Q.; Gossweiler, G. R.; Craig, S. L.; Zhao, X. Cephalopod-inspired design of electro-mechano-chemically responsive elastomers for on-demand fluorescent patterning. *Nat. Commun.* **2014**, *5*, 4899.

(26) Qiu, W.; Gurr, P. A.; da Silva, G.; Qiao, G. G. Insights into the mechanochromism of spiropyran elastomers. *Polym. Chem.* **2019**, *10*, 1650−1659.

(27) Chen, Y.; Zhang, H.; Fang, X.; Lin, Y.; Xu, Y.; Weng, W. Mechanical activation of mechanophore enhanced by strong hydrogen bonding interactions. *ACS Macro Lett.* **2014**, *3*, 141−145.

(28) Lee, C. K.; Beiermann, B. A.; Silberstein, M. N.; Wang, J.; Moore, J. S.; Sottos, N. R.; Braun, P. V. Exploiting force sensitive spiropyrans as molecular level probes. *Macromolecules* **2013**, *46*, 3746−3752.

(29) Gossweiler, G. R.; Kouznetsova, T. B.; Craig, S. L. Force-rate characterization of two spiropyran-based molecular force probes. *J. Am. Chem. Soc.* **2015**, *137*, 6148−6151.

(30) Barbee, M. H.; Kouznetsova, T.; Barrett, S. L.; Gossweiler, G. R.; Lin, Y.; Rastogi, S. K.; Brittain, W. J.; Craig, S. L. Substituent effects and mechanism in a mechanochemical reaction. *J. Am. Chem. Soc.* **2018**, *140*, 12746−12750.
(31) Raisch, M.; Genovese, D.; Zaccheroni, N.; Schmidt, S. B.; Focarete, M. L.; Sommer, M.; Gualandi, C. Highly Sensitive, Anisotropic, and Reversible Stress/Strain-Sensors from Mechanochromic Nanofiber Composites. *Adv. Mater.* **2018**, *30*, 1802813.
(32) Beiermann, B. A.; Davis, D. A.; Kramer, S. L. B.; Moore, J. S.; Sottos, N. R.; White, S. R. Environmental effects on mechanochemical activation of spiropyran in linear PMMA. *J. Mater. Chem.* **2011**, *21*, 8443−8447.
(33) Lee, C. K.; Diesendruck, C. E.; Lu, E.; Pickett, A. N.; May, P. A.; Moore, J. S.; Braun, P. V. Solvent Swelling Activation of a Mechanophore in a Polymer Network. *Macromolecules* **2014**, *47*, 2690−2694.
(34) Qiu, W.; Gurr, P. A.; Qiao, G. G. Regulating Color Activation Energy of Mechanophore-Linked Multinetwork Elastomers. *Macromolecules* **2020**, *53*, 4090−4098.

https://dx.doi.org/10.1021/acs.macromol.0c00985
Macromolecules 2020, 53, 7954−7961